

Photoproduction of $\Sigma^+ K_s^0$ with the CBELSA/TAPS-setup

Ralf Ewald
for the CBELSA/TAPS collaboration

Physics Institute, University of Bonn

Abstract. Albeit quark models explain the known baryon spectrum reasonably well, they all overpredict the number of states significantly. This is often called the "missing resonance" problem. It is speculated, that some of these resonances remained undetected in pi-induced reactions, but have a sizeable coupling to channels with strangeness involved. This provided our motivation to measure cross sections and polarisation observables in associated Kaon-Hyperon photoproduction with the focus on the $\Sigma^+ K_s^0$ channel. Up to now, for this particular channel only limited data exists from the SAPHIR-, CLAS- and CBELSA/TAPS-collaboration for total and differential cross sections, and for recoil polarisation. Using the linearly polarised, energy tagged photon beam at the ELSA particle accelerator of Bonn University, data were taken with the combined photon spectrometers Crystal Barrel and TAPS. This setup is well suited to detect multi photon final states and therefore ideal to measure the reaction channel $\gamma p \rightarrow \Sigma^+ K_s^0 \rightarrow p \pi^0 \pi^0 \pi^0 \rightarrow p 6\gamma$. Here the extraction of cross sections, the recoil polarisation P and the photon asymmetry Σ , which is measured for the first time, will be discussed.

Keywords: photoproduction, strangeness, polarisation observables, cross sections

PACS: 13.60.+r, 13.60.Hb, 13.88.+e, 14.20.Jn, 14.40.Df

INTRODUCTION

Photoproduction involving associated strangeness offers a great potential to study the nucleon spectrum. It is regarded as a possibility to get a hand on *missing resonances* ([1]) which couple only weakly to the πN channel. For the resonance identification it is a great advantage that the recoil polarisation P can be inherently determined through the weak decay. This single polarisation observable P is one of the 16 observables which describe the cross section for the production of one pseudoscalar meson. Fortunately, the observables are not independent from each other. Thus, only eight well-chosen observables have to be measured. These are four double polarisation observables, the unpolarised cross section, the target asymmetry, the photon asymmetry and the mentioned recoil polarisation. Therefore, a full description of a reaction channel or a so-called complete experiment can be accomplished with strangeness channels in the near future.

We investigate reaction channels involving associated strangeness production with the CBELSA/TAPS experiment at the electron stretcher facility ELSA in Bonn. We concentrate on the neutral decay channels of such reactions, since both main detectors are sensitive on photons. Here, results are given for the reaction channel $\gamma p \rightarrow \Sigma^+ K_s^0 \rightarrow p \pi^0 \pi^0 \pi^0 \rightarrow p 6\gamma$. We used a linearly polarised photon beam and an unpolarised target for the data sets I present here. In this case the cross section can be written in the form:

$$\frac{d\sigma}{d\Omega} = \frac{d\sigma}{d\Omega_0} (1 + \delta_l \Sigma \cos(2\phi) + P). \quad (1)$$

Here $\frac{d\sigma}{d\Omega_0}$ denotes the differential cross section in case of an unpolarised photon beam, Σ the photon asymmetry and P the recoil polarisation. δ_l announces the degree of linear polarisation of the photon beam and ϕ the angle between the polarisation plane and the reaction plane.

While the differential and total cross section and the recoil polarisation had been measured before for the reaction channel $\gamma p \rightarrow \Sigma^+ K_s^0$, the photon asymmetry Σ is determined for the first time.

EXPERIMENTAL SETUP

The data was taken with the CBELSA/TAPS experiment at the Bonn electron stretcher facility ELSA which provided a quasi-continuous electron beam with energies up to 3.2 GeV. The electron beam is converted into a linearly polarised photon beam via coherent bremsstrahlung off a diamond radiator. The resulting photon beam has a typical intensity of

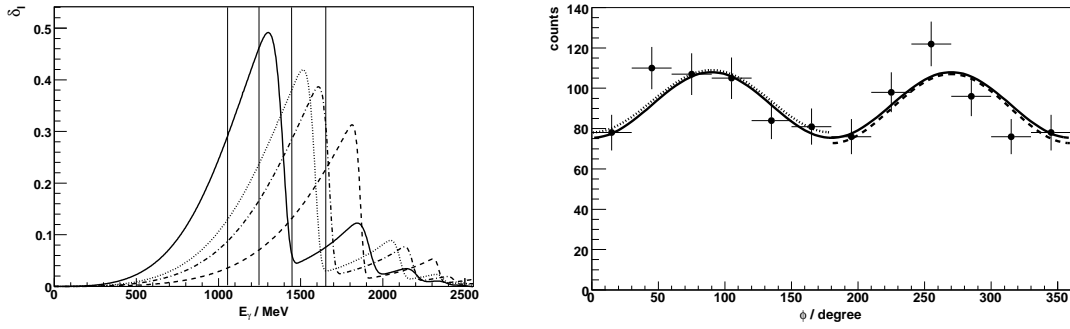


FIGURE 1. Left: The degree of linear polarisation for the four settings. The maximum degrees were 49% at $E_\gamma = 1305 \text{ MeV}$ (A), 42% at $E_\gamma = 1515 \text{ MeV}$ (B), 39% at $E_\gamma = 1610 \text{ MeV}$ (C) and 31% at $E_\gamma = 1814 \text{ MeV}$ (D). Vertical lines display the analysed energy range and binning. Right: Example of a measured ϕ distribution of the $\pi^0\pi^0$ final state is shown for the energy range $E_\gamma = (1550 \pm 100) \text{ MeV}$ and the angular range $0.6 < \cos(\theta_{CMS}) < 1$. The solid lines indicates the overall fit, the dotted and dashed line the separate fits to determine the systematic error.

10^7 photons per second and a degree of polarisation depending on the orientation of the diamond.

To obtain the energy of the emitted bremsstrahlung photons the momenta of the electrons were measured with a combination of a dipole magnet and a hodoscope consisting of 480 scintillating fibers and 14 scintillating bars behind them. This tagging system covered an energy range from 0.5 GeV to 2.55 GeV.

The photon beam hit a 5 cm long liquid-hydrogen target in the center of the Crystal Barrel calorimeter. The Crystal barrel consisted of 1290 CsI(Tl) crystals of 16 radiation lengths. In a cylindrical arrangement it covered polar angles from 30° to 168° with full azimuthal coverage. The forward cone was covered by the TAPS calorimeter which consisted of 528 BaF_2 crystals of 12 radiation lengths arranged as a hexagonal wall. It covered polar angles from 5° to 30° . Together, both calorimeters provided a geometrical acceptance of 99% 4π . Due to the high granularity and good acceptance this detector arrangement was well suited to measure multi photon final states.

To distinguish between charged and uncharged particles a cylindrical inner detector surrounded the target. It consisted of three layers of scintillating fibers. The probability that two out of three layers detect a charged particle was 98%. Charged particles emitted in forward direction were identified by 5mm thick plastic scintillators installed in front of the TAPS crystals. These VETO-counters had an efficiency of 80%.

To determine the photon flux a gamma intensity monitor was used. It consisted of 9 BaF_2 crystals arranged in a quadratic configuration. For a detailed description of the experimental setup, see [2].

For the discussed analysis, data was taken with four different diamond orientations. The degree of polarisation as a function of the incident photon energy for the four settings is shown in Figure 1.

DATA ANALYSIS

To extract the observables from the reaction channel $\gamma p \rightarrow \Sigma^+ K_s^0 \rightarrow p\pi^0\pi^0\pi^0 \rightarrow p6\gamma$, events are selected with six photons and, if measured, one proton in the final state. Therefore, there are three different event classes. In the first class events are inserted where only six photons are measured. In the second class all events with seven detected particles, but no identified proton, are collected. And in the third class events are summarized with six measured photons and one proton.

Then all possible $\gamma\gamma$ -combinations were build and the π^0 s selected via a cut on the $\gamma\gamma$ invariant mass.

To suppress the main background which arises from the reaction $\gamma p \rightarrow p\eta \rightarrow p\pi^0\pi^0\pi^0$, an anticut on the $\pi^0\pi^0\pi^0$ invariant mass is done. If the mass is between 460 MeV and 640 MeV the event is rejected. The cut is relatively wide to get rid of the large photon asymmetry of the $p\eta$ reaction channel.

To reduce the background furthermore and to improve the resolution, a kinematic fit with the hypothesis $\gamma p \rightarrow p\pi^0\pi^0\pi^0$ is performed. A measured proton is not demanded. It is calculated via energy and momentum conservation. To decide if a fit result is adequate, a cut on the confidence level is made. The level has to be higher than 0.1. For the first and third event class this can be done easily, because the proton is not measured or is identified and can

be excluded. For the second event class, with seven unidentified particles, all possible combinations run through the kinematic fit. All results which survive the cut on the confidence level are investigated further.

In case of the third event class, the calculated proton is compared to the measured proton. If the difference of the polar angles is greater than 8° or the azimuth angles deviate from each other more than 15° , the event is rejected. In case of the second event class, the calculated protons of the valid fit results are compared to their proton candidates. The same cut limits are chosen as for the third event class.

Now all possible $p\pi^0$ and $\pi^0\pi^0$ combinations are formed and a cut on the Σ^+ mass is made with cut limits of 1170 MeV and 1210 MeV.

After that the K_s^0 signals are obtained in all $\pi^0\pi^0$ invariant mass spectra. Every signal sits on top of a broad distribution which mainly consists of uncorrelatedly produced three π^0 s. Such events are simulated using the Monte Carlo-Simulation Geant3 and the generated background is subtracted from the measured data to get clear signals.

The acceptance for the reaction $\gamma p \rightarrow \Sigma^+ K_s^0 \rightarrow p\pi^0\pi^0\pi^0 \rightarrow p6\gamma$ is determined using the Monte Carlo-Simulation Geant3. The generated events are produced and saved in such a way that they can run through the same analysis. It turns out that the acceptance is independent from the polar and azimuth angles, but decreases slightly with increasing photon beam energy. The reason for the flat angular distributions is that the produced hyperons and kaons still decay into multi-particle final states. The total acceptance is roughly around 10%, even for the most forward and backward angles. This means that no extrapolations have to be made to extract the total cross section.

To extract the cross sections the data has to be normalised. The results which are presented here are normalised using the measured photon flux. The photon flux is determined with the tagging system and the gamma intensity monitor. The procedure is explained in [3].

The polarisation of the recoiled hyperon is determined by measuring the angle ψ between the emitted proton and the normal to the reaction plane. The $\pi^0\pi^0$ invariant mass spectra are separated into two regions of $\psi < 90^\circ$, where the proton is emitted in a direction pointing above the reaction plane, and $\psi > 90^\circ$, where the proton is flying in a direction below the reaction plane. For both regions the Kaon yields, N_{above} and N_{below} , are determined. The recoil polarisation is given by

$$P = \frac{2(N_{above} - N_{below})}{\alpha_0(N_{above} + N_{below})}. \quad (2)$$

$\alpha_0 = 0.98$ is the decay parameter taken from [4].

The photon asymmetry is extracted using the $\cos(2\phi)$ -dependency shown in equation 1. The fit

$$f(\phi) = A + B \cdot \cos(2\phi) \quad (3)$$

is performed on the ϕ distribution of the $\pi^0\pi^0$ combinations after all cuts for each bin. The photon asymmetry is given by $\Sigma = -\frac{B}{A \cdot \delta_\phi}$. An example of a ϕ distribution is shown in Figure 1. The effect of the photon asymmetry clearly shows up as a modulation in ϕ . To get the systematic error the regions $\theta < 180^\circ$ and $\theta > 180^\circ$ are fitted separately. For an ideal detector setup the fit results should be the same. Taken in account statistic fluctuations, divergences greater than 1σ were counted as the systematic error of the measurement.

RESULTS

Figure 2 shows on the left side the results, denoted by circles, for the differential cross section for 12 energy bins, each 100 MeV wide. The error bars are purely statistically, the systematic errors are given by the columns. The results are compared to the results of SAPHIR (squares, [5]) and previous CBELSA/TAPS (triangles, [6]). The previous CBELSA/TAPS results are extracted from data taken with an unpolarised photon beam; in addition, the differential cross sections are normalised using the reaction $\gamma p \rightarrow p\eta$. So, the photon flux was not measured directly. All three data sets are in good agreement and are well-described by the Bonn-Gatchina-PWA (solid line, [1]). But the Kaon-MAID model (dotted line, [7]) fails in reproducing the data. Beside the overestimation of the amplitude of the cross section, it claims a rise in the backward region and cannot reproduce the drop in the cross section in forward direction around 1800 MeV photon beam energy. Reducing the contributions of the Born terms and the $S_{31}(1900)$ removes the problems of the overestimated amplitude and the rising in the backward region. The obtained values are $|g_{KSN}| = 0.7$, $|G_1| = 0.3$ and $|G_3| = 0.3$. The drop in the cross section could possibly be explained with t-channel-contributions. The vector meson $K^*(892)$ is an important exchange particle in the reaction below 1800 MeV beam photon energy. Above this energy value the $K^*(892)$ is produced as a free particle and its contribution to the cross section as an exchange particle vanishes. Such processes are known from the $p\pi$ -reaction channels as well. This leads us to modify the Kaon-MAID

model (dashed line) which then describes the measured CBELSA/TAPS data pretty well.

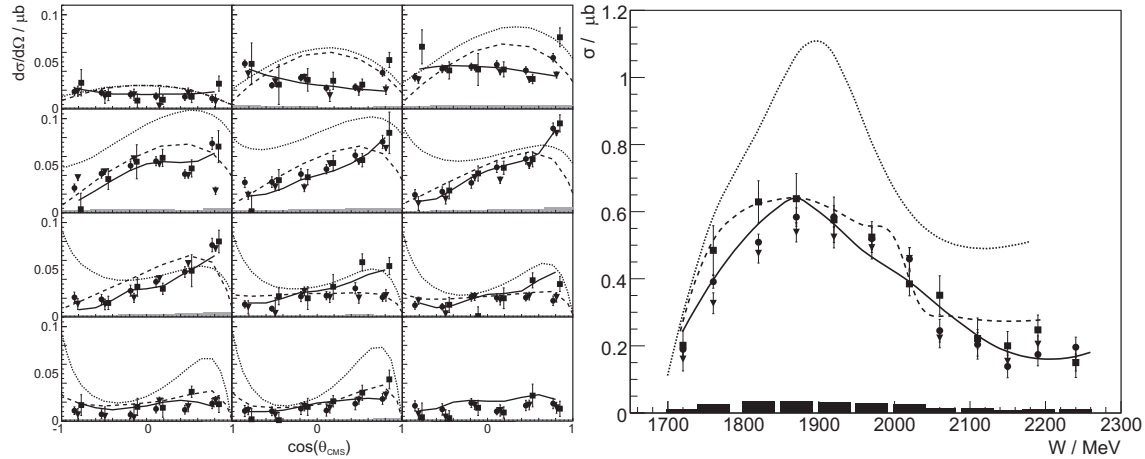


FIGURE 2. Results (dots) for the differential (left side) and the total (right side) cross section are compared to published CBELSA/TAPS data (triangles) and SAPHIR data (squares). The dotted line shows the standard Kaon-Maid model prediction, the dashed line that of the modified Kaon-Maid model and the solid line indicates that of the Bonn-Gatchina-PWA. The differential cross section is measured for 12 beam photon energy bins from 1050 MeV to 2250 MeV, each 100 MeV wide.

The same can be said for the total cross section. Again the results are in a good agreement to the published data and is well described by the Bonn-Gatchina-PWA. This is shown in Figure 2 on the right side. The symbols are the same as before. And again the standard Kaon-MAID model overpredicts the cross section, but the modified model is able to describe the experimental data.

The result for the recoil polarisation is shown in Figure 3 (left) in comparison to the published CBELSA/TAPS data. In respect to the big error bars both measurements are in good agreement. Here, the standard Kaon-MAID model and the modified model cannot describe the data at all. To compare the result to the SAPHIR data, the data of the present experiment is rebinned. This is shown in Figure 3 on the right. There is no difference seen between both experimental results.

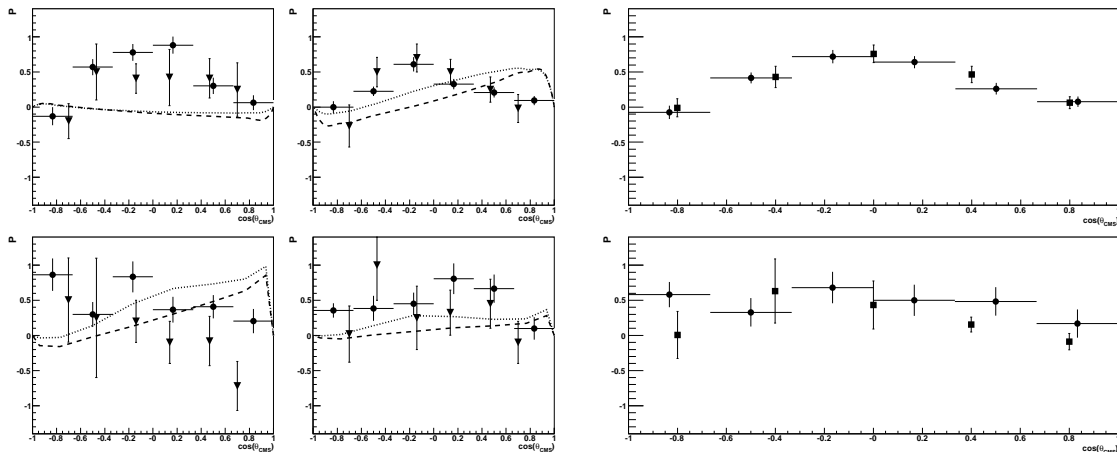


FIGURE 3. Results (dots) for the recoil polarisation P are compared to published CBELSA/TAPS data (triangles, on the left) for four beam photon energy bins (Left to right: $E_\gamma = (1200 \pm 150)MeV$, $E_\gamma = (1500 \pm 150)MeV$, $E_\gamma = (1800 \pm 150)MeV$, $E_\gamma = (2100 \pm 150)MeV$.) and SAPHIR data (squares, on the right) for two beam photon energy bins (top: $E_\gamma = (1300 \pm 250)MeV$, bottom: $E_\gamma = (1900 \pm 350)MeV$.). The dotted line shows the standard Kaon-Maid model prediction, the dashed line that of the modified Kaon-Maid model.

The extracted values for the photon asymmetry Σ is shown in Figure 4 for three beam photon energy bins, each 200 MeV wide. Here, the experimental data is well described by both Kaon-MAID models. The photon asymmetries, depicted as a function of $\cos(\theta_{CMS})$ of the Kaon, can be of the order of 70%. The large negative photon asymmetry in

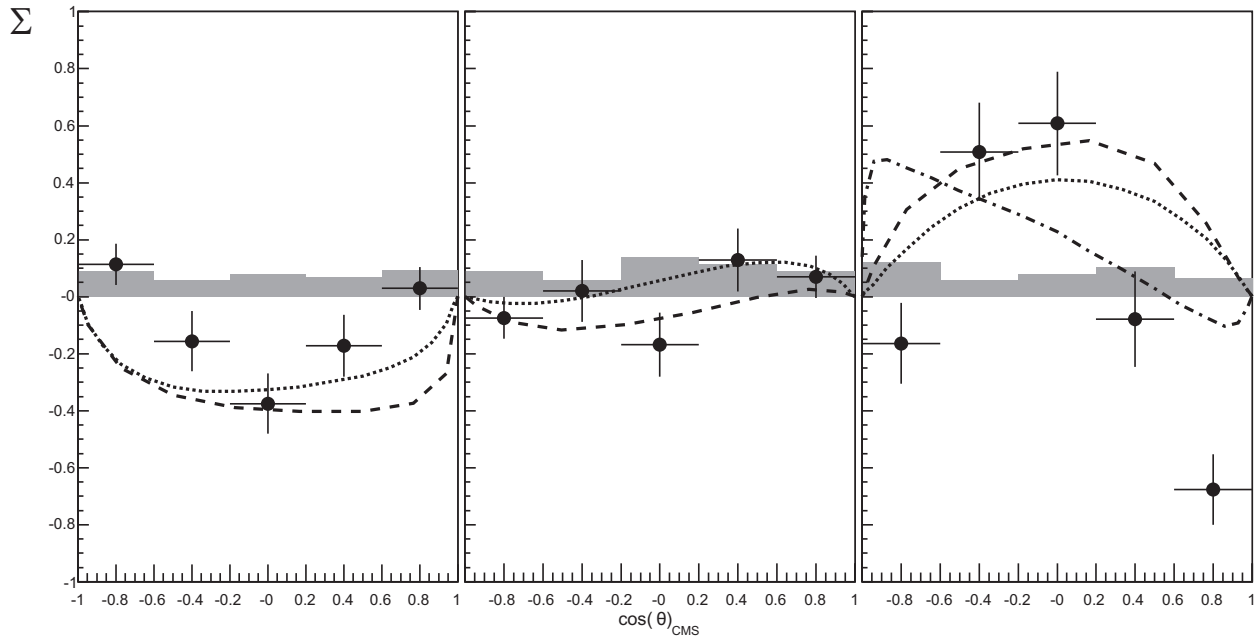


FIGURE 4. The measured photon asymmetry Σ as a function of $\cos(\theta_{CMS})$ of the K_s^0 for three beam photon energy bins. Left to right: $E_\gamma = (1150 \pm 100)MeV$, $E_\gamma = (1350 \pm 100)MeV$ and $E_\gamma = (1550 \pm 100)MeV$. The dotted line indicates the standard Kaon-MAID model prediction, the dashed line represents the modified Kaon-MAID model and the dashed-dotted line the modified Kaon-MAID model with a more favored $K^1(1270)$ t-channel-exchange.

forward direction for a high beam photon energy could be a hint that the vector meson exchange of the $K^1(1270)$ is prominent there (dashed-dotted line).

SUMMARY

The differential and total cross section, the recoil polarisation P and the photon asymmetry Σ for the reaction $\gamma p \rightarrow \Sigma^+ K_s^0$ have been measured with the CBELSA/TAPS experiment at ELSA. Our new data agrees well with previous measurements of the cross section and recoil polarisation. The photon asymmetry has been measured for the first time. The Kaon-MAID model fails to describe the measurements. In a modified model t-channel-processes can explain the characteristics of the reaction. This suggests that the contributions of such processes could be big. It should be investigated further.

This work was supported by the Deutsche Forschungsgemeinschaft (DFG) within the SFB/TR16.

REFERENCES

1. A. V. Sarantsev et al., *Eur. Phys. J. A* **25**, 427 (2005).
2. D. Elsner et al., *Eur. Phys. J. A* **33**, 147 (2007).
3. K. Fornet-Ponse, *Die Photonmarkierungsanlage für das Crystal Barrel/TAPS-Experiment an ELSA*, Ph.D. thesis, Bonn University, Bonn, Germany (2009).
4. P. D. Group, *Particle Physics Booklet*, Institute of Physics PUBLISHING, CERN, Geneva, Switzerland, 2006.
5. R. Lawall et al., *Eur. Phys. J. A* **24**, 275 (2005).
6. R. J. J. Castelijns et al., *Eur. Phys. J. A* **35**, 39 (2008).
7. Kaon-MAID, <http://www.kph.uni-mainz.de/MAID/> (2007).